

Rare earth element–SiO₂ systematics of island arc crustal amphibolite migmatites from the Asago body of the Yakuno Ophiolite, Japan: a field evaluation of some model predictions

Xiaofei Pu · James G. Brophy · Tatsuki Tsujimori

Received: 25 April 2014 / Accepted: 21 August 2014
© Springer-Verlag Berlin Heidelberg 2014

Abstract The two most commonly invoked processes for generating silicic magmas in intra-oceanic arc environments are extended fractional crystallization of hydrous island arc basalt magma or dehydration melting of lower crustal amphibolite. Brophy (Contrib Mineral Petrol 156:337–357, 2008) has proposed on theoretical grounds that, for liquids >~65 wt% SiO₂, dehydration melting should yield, among other features, a negative correlation between rare earth element (REE) abundances and increasing SiO₂, while fractional crystallization should yield a positive correlation. If correct, the REE–SiO₂ systematics of natural systems might be used to distinguish between the two processes. The Permian-age Asago body within the Yakuno Ophiolite, Japan, has amphibolite migmatites that contain felsic veins that are believed to have formed from dehydration melting, thus forming an appropriate location for field verification of the proposed REE–SiO₂ systematics for such a process. In addition to a negative correlation between liquid SiO₂ and REE abundance for liquids in excess of ~65 % SiO₂, another important model feature is that, at very high SiO₂ contents (75–76 %), all of the REE should have abundances less than

that of the host rock. Assuming an initial source amphibolite that is slightly LREE-enriched relative to the host amphibolites, the observed REE abundances in the felsic veins fully support all theoretical predictions.

Keywords Amphibolite · Migmatite · Rare earth elements · Partial melting · Silicic magma

Introduction

The generation of silicic magmas in intra-oceanic arc environments is a subject that has received a lot of attention. Though many possible origins have been suggested, the two most commonly invoked processes for generating such magmas are extended fractional crystallization of hydrous, mantle-derived island arc basalt (IAB) magma or dehydration melting of lower crustal amphibolite. As is often the case, when two different processes are suggested for the same phenomenon, both processes are probably occurring. In a former study, Brophy (2008) proposed that the REE–SiO₂ systematics of mafic to felsic magmas in oceanic arc environments could be used to distinguish between these two processes in natural arc lavas and/or intrusives. Because the 2008 study was entirely model based, it requires some form of field verification before REE–SiO₂ systematics can be accepted as a useful geochemical tool. The present study consists of a petrologic and geochemical study of a natural example of partial melting of island arc crust from the Asago Body within the Yakuno ophiolite located on Honshu Island, Japan (Fig. 1). The goal of the study is to evaluate the proposed REE–SiO₂ systematics of Brophy (2008) for dehydration melting of lower crustal amphibolite. The Yakuno migmatites were first studied by Suda (2004) who concluded that they were generated by dehydration melting of island arc crustal amphibolite.

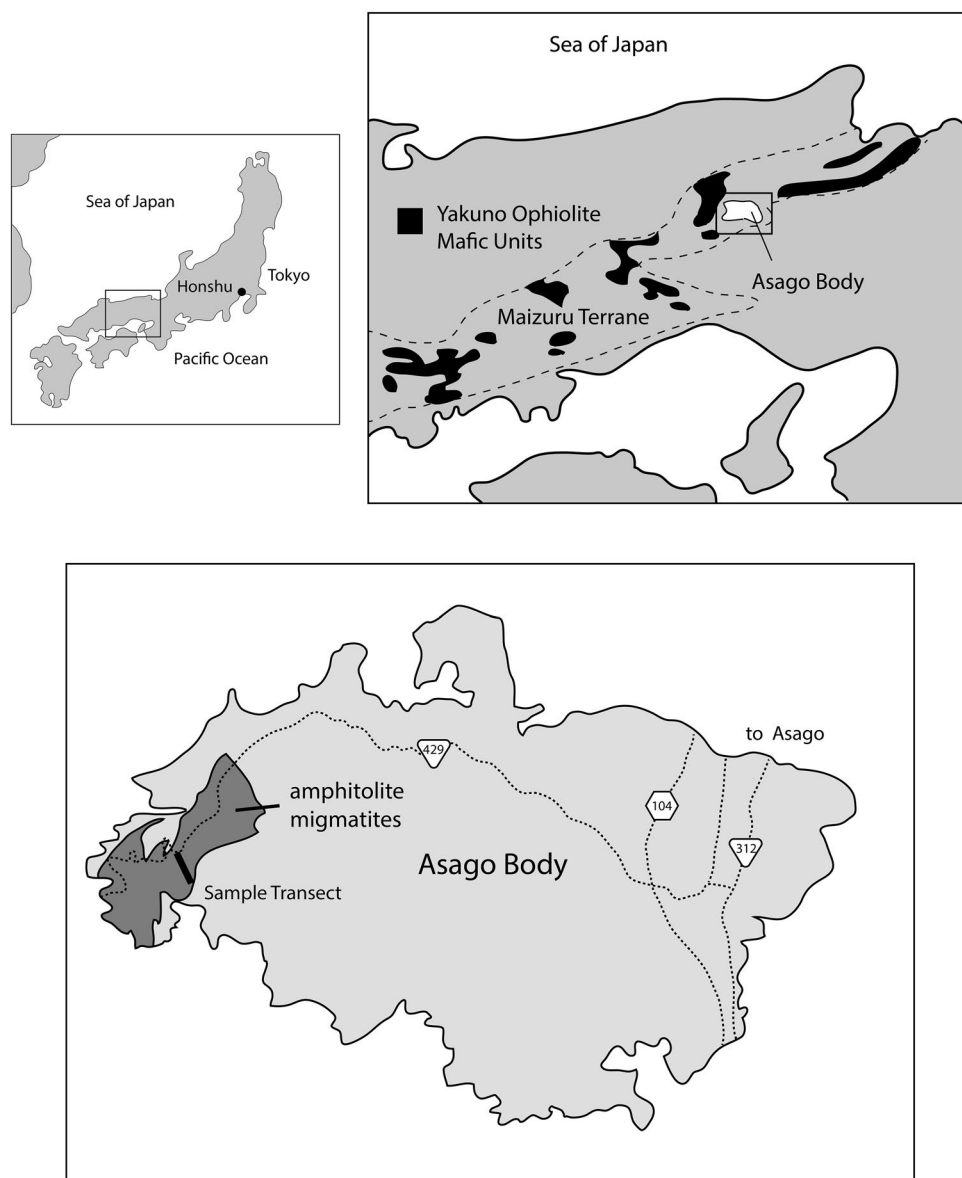
Communicated by T. L. Grove.

X. Pu · J. G. Brophy (✉)
Department of Geological Sciences, Indiana University,
Bloomington, IN 47405, USA
e-mail: brophy@indiana.edu

X. Pu
e-mail: pux@indiana.edu

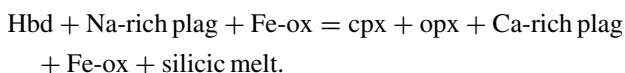
T. Tsujimori
The Pheasant Memorial Laboratory for Geochemistry
and Cosmochemistry (PML), Institute for Study of the Earth's
Interior, Okayama University, Misasa, Tottori-Ken 682-0193,
Japan
e-mail: tatsukix@misasa.okayama-u.ac.jp

Fig. 1 Generalized map showing the location of the Asago Body in the Yakuno Ophiolite (dark colored mafic units) and the amphibolite migmatites that are the focus of this study (after Suda 2004)



REE–SiO₂ systematics for amphibolite melting and basalt fractionation in oceanic island arcs

It is commonly assumed that amphibolite melting is simply the reverse process of basalt fractionation, and therefore, the two processes cannot be distinguished from one another on chemical grounds. This is not true. During the dehydration melting of amphibolite, silicic melts are generated by one or more reactions of the type shown below (Rushmer 1991; Beard and Lofgren 1991; Rapp and Watson 1995)



This reaction will continue to produce silicic melt until all of the original hornblende is consumed. Thus, the REE–SiO₂ systematics of the silicic melt will always

be controlled by the combined presence of hornblende, plagioclase, orthopyroxene and clinopyroxene. During fractional crystallization of hydrous, IAB magma, hornblende is most likely present as a crystallizing phase in the lower crust (Davidson et al. 2007), but the extent to which it is a significant crystallizing phase is still uncertain (e.g., Davidson et al. 2013). Thus, in many arc systems, extended basalt fractionation may be dominated by olivine, clinopyroxene, orthopyroxene and Fe-oxide, but not hornblende. From the standpoint of REE–SiO₂ systematics, the potentially different role played by hornblende in dehydration melting of amphibolite and extended IAB fractionation may be very significant. The reason for this is emphasized in Fig. 2, which shows the variation in hornblende-liquid *D* values [plotted as log(*D*)] versus liquid SiO₂ for La and Yb. For both elements, there is a steady

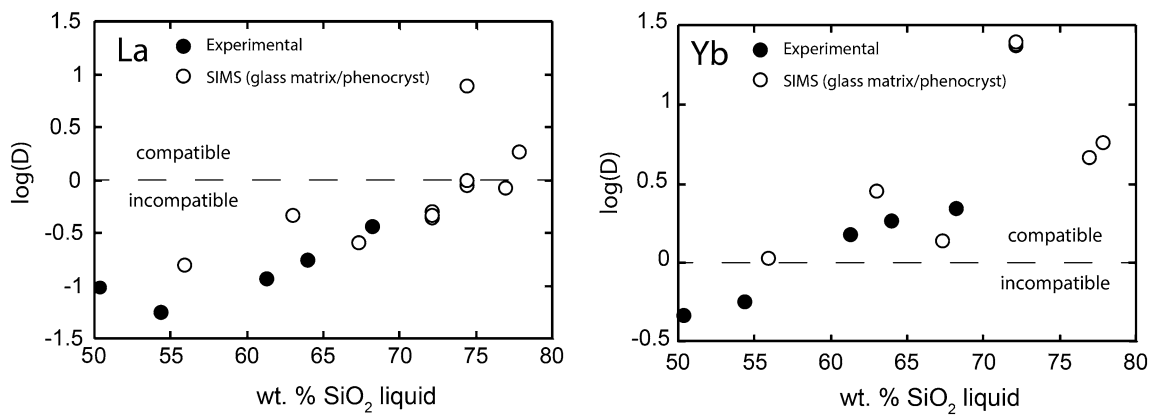
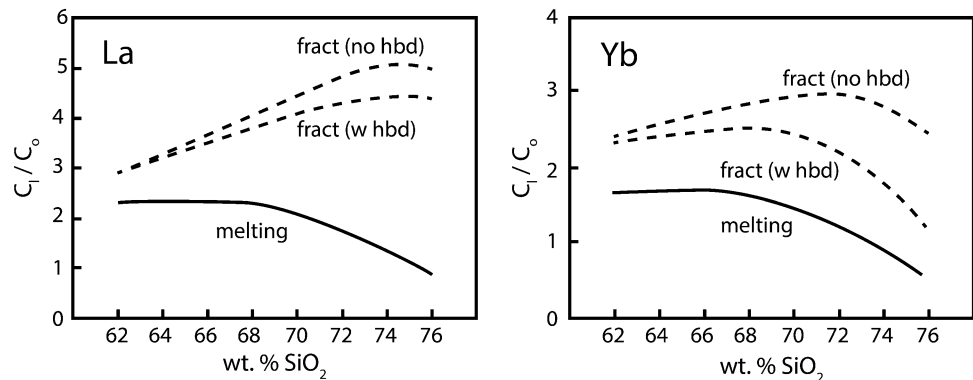


Fig. 2 Hornblende–liquid La and Yb D values versus SiO_2 content of co-existing liquid (glass). Data sources include Sisson (1994), Klein et al. (1997), Dalpe and Baker (2000) and Brophy et al. (2011)

Fig. 3 Predicted REE– SiO_2 variations (from Brophy 2008) for lower crustal amphibolite melting, hornblende-free mid-crustal fractionation of basalt and hornblende-bearing mid-crustal fractionation of basalt



increase in $\log(D)$ and therefore D with increasing liquid SiO_2 . Furthermore, the partitioning behavior eventually changes from incompatible ($D < 1$) to compatible ($D > 1$). For La, this switch occurs at around 75 wt% SiO_2 , but reaches as low as ~60 % SiO_2 for Yb. Of the four minerals mentioned above (olivine, plagioclase, clinopyroxene and hornblende), hornblende is the only one that displays this behavior to such a large extent. What this means is that, for SiO_2 -rich liquids, the presence or absence of hornblende can translate into dramatically different partitioning behavior for the REE.

Brophy (2008) modeled the variation in La and Yb with increasing liquid SiO_2 for both fractional crystallization of IAB basalt and dehydration melting of lower arc crust amphibolite. The modeling combined major element mass-balanced fractional crystallization models and experimentally based amphibolite melting models with quantitative expressions describing the $\log(D)$ – SiO_2 variations for La and Yb shown in Fig. 2. The results are summarized in Fig. 3, which shows the predicted variation in La and Yb abundances for batch melting of amphibolite and fractional crystallization of IAB basalt. Fractional melting

and accumulated fractional melting show similar overall results and are not shown here. In both cases, the initial gabbro or basalt was assumed to contain 50 wt% SiO_2 . The results are expressed in terms of an element enrichment factor in the liquid, C_1/C_0 , where C_1 is the concentration of the element in the liquid and C_0 is the original concentration of the element in the source rock (for melting) or the original basalt magma (for crystallization). The most important feature of Fig. 3 is that, for liquids in excess of ~65 % SiO_2 , amphibolite melting reveals a *negative* correlation between La and Yb abundances and SiO_2 content, while IAB basalt fractionation shows a *positive* correlation up to SiO_2 contents of around 70 wt% after which a negative correlation is observed. These differences reflect (1) the increasing compatibility of La and Yb in hornblende with increasing liquid SiO_2 and (2) the dominant role played by hornblende during melting and the minor role during crystallization. If these model predictions are correct, then they could provide an important geochemical tool for distinguishing between a melting and fractional crystallization origin for natural silicic lavas in intra-oceanic arc environments.

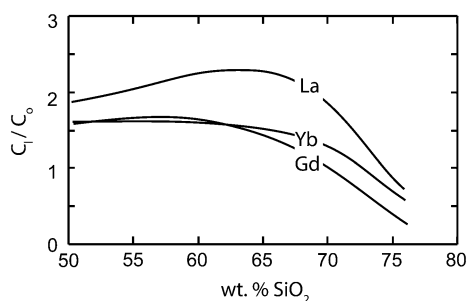


Fig. 4 Predicted variations in liquid enrichment factors (C_l/C_0) for La (HREE), Gd (MREE) and Yb (HREE) from the model of Brophy (2008)

Predicted REE–SiO₂ systematics for amphibolite melting

The most controversial part of the Brophy (2008) modeling is the predicted REE–SiO₂ systematics for amphibolite melting, the field verification of which constitutes the essence of the current study. The gist of the predicted systematics is summarized in Fig. 4, which shows predicted liquid enrichment factors (C_l/C_0) for representative light (La), middle (Gd) and heavy (La) rare earth elements (REEs) as a function of liquid SiO₂ content. Two major predictions can be made. First, for liquids greater than around 65 % SiO₂, all of the REE should show a negative correlation with increasing liquid SiO₂. Second, at very high liquid SiO₂ contents (around 75–76 %), the LREE should all show enrichment values <1. It is these two theoretical predictions that are to be evaluated in this study.

Analytical methods

Bulk rock major and trace element analyses were conducted by XRF and LA-ICPMS at Michigan State University following analytical procedures described in Deering et al. (2008). Major element compositions of minerals were determined by electron microprobe analysis (EMPA) on a Cameca SX50 located at Indiana University. Operating conditions included a 15 kV acceleration voltage, 20 nA sample current and a beam diameter of 3 microns. Na₂O was always analyzed first to reduce any effects of volatilization/diffusion. Accessory mineral percentages in the mafic amphibolite were determined by initial EMPA of individual minerals followed by image analysis of multiple (15) back scatter electron images for four different amphibolite samples.

The Yakuno Ophiolite

The Permian-aged Yakuno Ophiolite is located on Honshu Island, Southwest Japan (Fig. 1). Three different segments have



Fig. 5 Field photograph showing one of the amphibolite migmatite outcrops that are the focus of this study

been identified within the ophiolite including unusually thick oceanic crust, island arc crust and oceanic back-arc basin crust (Ishiwatiri 1985; Hayasaka 1990; Ichiyama and Ishiwatiri 2003). The Asago body is a fault-bounded tectonic slice within the ophiolite suite. It is comprised of three structural units: a Lower Unit (L-Unit), Middle-Unit (M-Unit) and Upper-Unit (U-Unit) (not shown in Fig. 1). The M-Unit is thought to represent a lower to middle crustal section of an intra-oceanic island arc (Hayasaka 1990). The amphibolite migmatites sampled for this study were located in the lower part of the M-Unit, near the boundary of the M- and L-Unit (Suda 2004). They were collected along a short southwesterly transect following the bottom of a small stream valley (Fig. 1). A total of ten samples were collected. Two samples represent mafic amphibolites without felsic veins, while the rest of the samples consist of intermixed mafic amphibolite and felsic veins. According to Suda (2004), the *P–T* conditions during the formation of these migmatites are estimated to be around 850 °C and 3.5–5.5 kbar with a peak metamorphic grade of granulite facies.

Sample description

The amphibolites show a clear migmatite signature with felsic veins and pockets dispersed throughout the amphibolite host (Fig. 5). The contacts between the mafic amphibolite host and the felsic material are always sharp, suggesting that the felsic melts were actually generated elsewhere and intruded into their current position through joints and fractures in the host rock. The scale and shape of the felsic intrusions vary from sample to sample. The amphibolite host consists of primary amphibole, plagioclase and minor amounts of augite. Detailed analysis of multiple samples indicates very small volumes of sphene (0.5 wt%), apatite

(0.15 wt%) and zircon (0.05 wt%). The amphibole is calcic and ranges from magnesio-hornblende to ferro-hornblende (Leake et al. 1997). The plagioclase has been extensively albitized with some crystals reaching Ab₁₀₀ in composition. Most crystals show some degree of saussuritization. A few plagioclase grains have compositions around Ab₃₅, suggesting that the original (pre-albitized) plagioclase was of this general composition. Augite is largely unaltered and compositionally uniform at around Wo₄₆En₃₆Fs₁₈. Secondary minerals include actinolite, prehnite, epidote, chlorite and saussurite minerals. Actinolite, though present in only small amounts, can partially or completely replace hornblende. Hornblende is occasionally replaced by chlorite. Small amounts of epidote and prehnite occur as discrete crystals.

The felsic veins consist of primary plagioclase and quartz. Quartz shows up as aggregates of fine-grained crystals and or intergrowths with plagioclase. Individual plagioclase crystals are still recognizable under cross-polar in microscope, but they have been mostly saussuritized. Most plagioclase crystals have been completely albitized (Ab₉₉–Ab₁₀₀). Subhedral hornblende xenocrysts can be found floating in the felsic material.

The hydrous secondary minerals in both the amphibolite and felsic intrusions point toward a significant prehnite to greenschist facies retrograde metamorphism that post-dated the peak metamorphic event (when partial melting occurred) by some undetermined amount of time.

Whole rock geochemistry

Whole rock major and trace element data are listed in Table 1. Total iron is reported as FeO*. SiO₂ contents (on an anhydrous basis) range from 47 to 55 % in the mafic amphibolites and from 76 to 81 % in the felsic intrusion samples. Figure 6 shows Harker variation diagrams for selected oxides. Within both the mafic and felsic groups, Al₂O₃, TiO₂, FeO*, MgO and CaO steadily decrease with increasing SiO₂, while Na₂O and K₂O show a rough increase with increasing SiO₂.

Figure 7 shows a chondrite-normalized trace element spider diagram for both mafic and felsic samples using the normalization factors of McDonough and Sun (1995). The mafic and felsic samples have similar overall patterns, but the felsic samples are enriched in the incompatible elements and depleted in the compatible elements compared with the mafic samples. The overall patterns are flat with several important anomalies including positive Ba, slightly negative Nb and Ti, and strong P depletion. Also seen are positive Ba anomalies more negative Ti (mostly in felsic samples) and Nb anomalies. Felsic samples have higher incompatible element abundances and lower compatible element abundances compared with the mafic samples.

The overall flat patterns in the chondrite-normalized profiles and the presence of positive Ba and negative Nb and Ti anomalies are consistent with an island arc setting as originally suggested by Hayasaka (1990) and Suda (2004).

Figure 8 shows chondrite-normalized REE patterns for both the mafic and felsic samples. The patterns for the mafic samples are flat with general abundances ranging from about 6 to 20 times those of chondrite. The patterns for the felsic samples are somewhat fractionated and concave upwards. Relative to the mafic samples, the inclined patterns for the felsic samples have resulted primarily from HREE depletion with only slight LREE enrichment.

Relationship between amphibolite host and felsic veins

Two important questions for this study are (1) do the felsic veins represent partial melts of amphibolite and; (2) do the felsic veins represent in situ partial melting of the amphibolites in which they are hosted? Several lines of evidence support an amphibolite melting origin for the felsic veins. First, the field relations are those of a classic migmatite, which are almost universally viewed as representing partial melting (e.g., Sawyer 2008). Second, relative to the host amphibolites, the felsic veins show slight LREE enrichment and significant HREE depletion. Furthermore, the HREE display a concave upwards pattern. This pattern is entirely consistent with melting of a source rock that contained significant residual hornblende at the time of melt extraction (i.e., an amphibolite). Finally, Fig. 9 compares the major element chemistry of the host amphibolites and felsic veins with the experimental melts of Beard and Lofgren (1991) for the dehydration melting of amphibolite over a pressure range of 3–6.9 kbar. All of the felsic veins have SiO₂ contents that are greater than the most SiO₂-rich experimental liquid. However, for all of the oxides, the felsic veins lie on extensions of the experimental liquid trends. When taken together, these three lines of reasoning strongly support an amphibolite melting origin for the felsic veins.

It is noteworthy that all of the felsic samples display a significant positive Eu anomaly (Fig. 8), the origin of which is unclear. Plagioclase preferentially retains Eu²⁺, while hornblende and augite preferentially exclude Eu²⁺ (e.g., Brophy et al. 2011). Thus, the positive anomaly could be a result of plagioclase accumulation, suggesting a fractional crystallization origin for the silicic veins, or partial melting of amphibolite wherein the silicic melt is in equilibrium with hornblende and/or augite during the melting process. Because there is so much field and textural evidence suggesting a partial melting origin, the positive Eu anomalies are most likely a reflection of the latter.

Several lines of evidence also suggest that the host amphibolites do not represent the true source rock for the

Table 1 Whole rock major and trace element data

Sample	14-M	16-M	15-M	17-M	13-M	20-M	12-M	19-M	18-F	17-F	11-F	20-F
SiO ₂	43.18	45.7	47.21	48.33	48.35	49	51.2	52.7	74.93	76.85	77.2	78.76
TiO ₂	1.15	1.44	1.32	1.23	0.94	1.15	0.59	1.25	0.18	0.26	0.02	0.04
Al ₂ O ₃	15.34	15.93	15.92	16.47	16.78	15.4	14.17	13.8	13.16	11.62	13.29	11.13
FeO _T	14.55	10.83	9.68	9.46	10.13	10.52	8.54	8.38	1.03	1.37	0.08	0.22
MnO	0.18	0.18	0.18	0.16	0.16	0.17	0.17	0.17	0.02	0.02	0	0.01
MgO	7.39	6.64	6.18	6.15	5.74	6.7	8.36	5.61	0.31	0.67	0.01	0.02
CaO	9.06	9.4	11.7	10.17	8.05	8	9.52	9.04	2.9	2.53	2.21	1.96
Na ₂ O	1.93	3.1	2.86	3.25	3.49	3.5	2.68	4.35	4.81	4.02	4.88	5.06
K ₂ O	0.48	0.61	0.46	0.52	0.83	0.97	0.77	0.45	0.38	0.31	0.64	0.18
P ₂ O ₅	0.02	0.19	0.18	0.18	0.1	0.13	0.08	0.16	0.03	0.02	0.01	0.01
LOI	5.04	4.67	3.14	2.91	4.22	3.17	2.86	3.06	2.07	2.12	1.59	2.55
Total	98.32	98.69	98.83	98.83	98.79	98.71	98.94	98.97	99.82	99.79	99.93	99.94
Ni	15	64	56	68	27	67	86	51	bd	bd	bd	bd
Cu	92	64	28	25	40	19	29	67	42	6	6	1
Zn	56	87	72	71	78	83	61	57	bd	bd	bd	bd
Rb	10	7	6	6	11	14	11	9	6	4	7	bd
Sr	158	413	458	568	315	407	252	252	309	326	299	219
Zr	15	81	76	56	93	86	36	61	150	137	23	59
Ba	125.4	131.6	110.5	108.5	208.8	253.9	151.6	11.7	115.3	91.5	197.7	79.5
La	1.06	5.3	4.45	4.57	8.07	4.92	4.25	5.01	10.46	7.1	8.76	11.57
Ce	2.83	14.63	12.58	13.1	21.48	14.04	9.52	12.82	21.92	13.92	18.76	24.53
Pr	0.43	2.43	2.06	2.21	3.24	2.28	1.24	1.36	1.92	1.18	1.74	2.42
Nd	2.39	12.48	10.62	11.87	15.41	11.66	5.66	5.17	6.07	3.56	5.78	8.43
Sm	0.77	3.68	3.23	3.65	4.24	3.57	1.59	1.06	0.98	0.41	0.79	1.48
Eu	0.39	1.25	1.12	1.24	1.1	1.13	0.62	0.96	0.73	0.66	0.47	0.34
Gd	1.14	4.48	3.97	4.36	4.82	4.2	2.01	1.1	0.96	0.36	0.8	1.13
Y	9.21	34.02	29.28	32.74	38.84	33.27	16.73	7.7	8.7	1.5	3.94	4.18
Dy	1.38	5.16	4.49	4.94	5.68	4.89	2.46	1.07	1.03	0.22	0.42	0.72
Ho	0.32	1.13	0.99	1.08	1.25	1.06	0.57	0.23	0.26	0.06	0.06	0.13
Lu	0.14	0.45	0.39	0.43	0.56	0.45	0.27	0.12	0.2	0.07	0.04	0.09
Yb	0.88	3.02	2.69	2.95	3.77	3.09	1.78	0.74	1.2	0.31	0.21	0.55
Tb	0.21	0.8	0.71	0.78	0.87	0.76	0.38	0.17	0.18	0.05	0.05	0.15
V	827	327	306	319	321	306	256	32.9	9.88	35.89	4.49	6.02
Cr	24.65	184.2	161.4	174.3	40.6	169	389.2	6.8	4.98	17.38	3.04	3.23
Nb	0.5	2.21	1.94	1.87	2.35	2.37	1.1	2.46	3.89	2.8	1.25	0.77
Hf	0.53	2.31	2.03	1.82	2.55	2.28	1.14	2.82	3.19	3.01	0.59	2.65
Ta	0.28	0.14	0.13	0.15	0.18	1.18	0.13	0.27	0.62	0.54	5.47	0.67
Pb	0.62	1.26	1.15	1.38	1.82	1.04	1.09	4.81	9.49	4.9	7.11	1.2
Th	0.15	0.12	0.16	0.14	0.23	0.12	0.75	0.17	2.34	0.5	2.67	6.15
U	0.05	0.07	0.07	0.08	0.1	0.08	0.25	0.13	0.74	0.12	0.74	0.86

bd Below detection limit

felsic veins and that the veins were generated elsewhere (presumably deeper) and then intruded into the current host rocks. First, the contacts between the felsic veins and host amphibolite are universally sharp, which is inconsistent with in situ partial melting (e.g., Sawyer 2008). Secondly, the host amphibolites are dominated by hornblende with only very small amounts of augite. Given that augite is a major reaction product during amphibolite melting, the

abundance of hornblende and lack of augite argue against partial melting in the host amphibolites.

Modeling REE–SiO₂ systematics

The REE–SiO₂ systematics for partial melting of the Asago body amphibolites was modeled using the same procedure

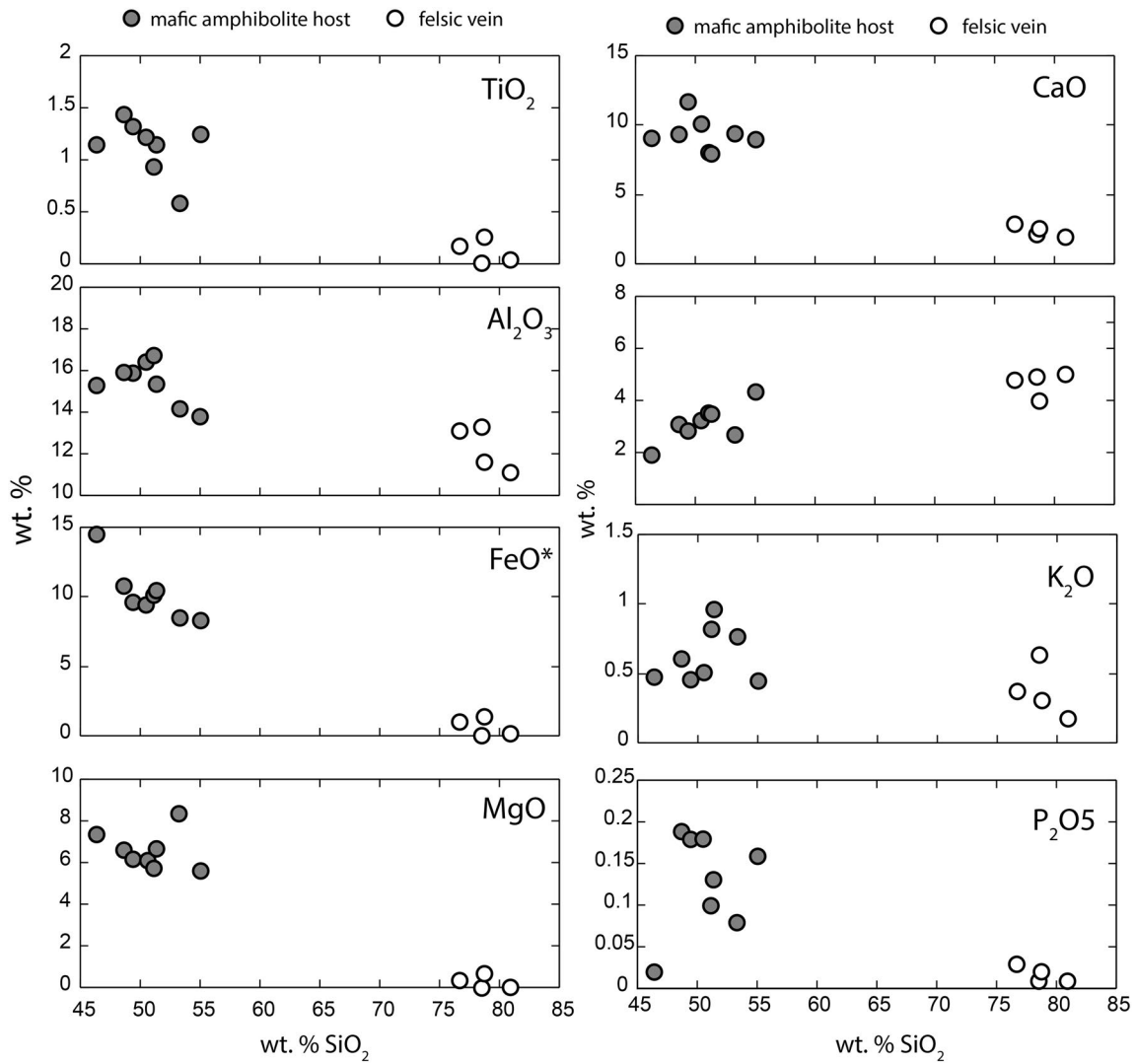


Fig. 6 Harker variation diagrams showing the mafic amphibolite hosts (*filled circles*) and felsic veins (*open circles*)

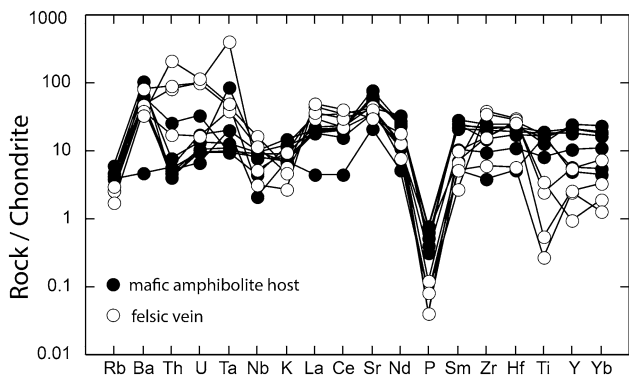


Fig. 7 Chondrite-normalized spider diagram for both the mafic amphibolite hosts (*filled circles*) and felsic veins (*open circles*)

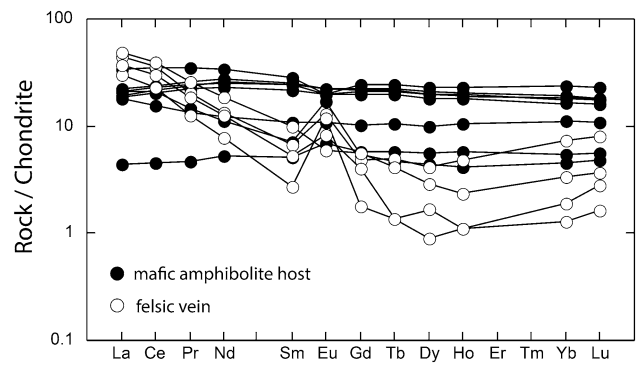


Fig. 8 Chondrite-normalized REE diagram for both the mafic amphibolite hosts (*filled circles*) and felsic veins (*open circles*)

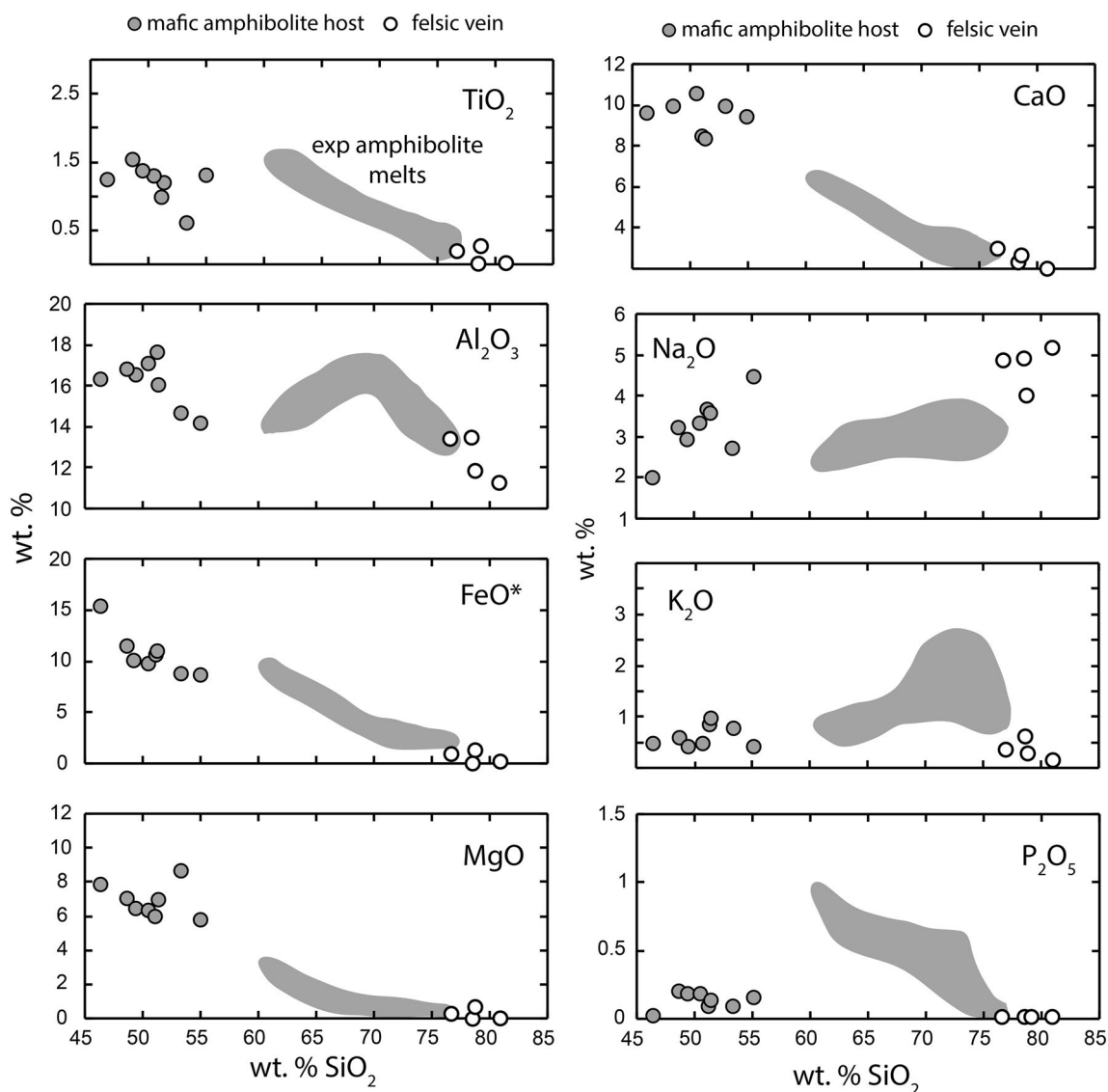


Fig. 9 Comparison of the mafic amphibolite hosts (filled circles) and felsic veins (open circles) with experimental glasses (gray fields) generated by the dehydration melting of natural amphibolites at pressures of 3–6.9 kb (Beard and Lofgren 1991)

employed by Brophy (2008). As described previously, a numerical amphibolite melting model based on existing experimental data was combined with liquid SiO_2 -dependant REE partition coefficients to calculate model liquid REE abundances as a function of liquid SiO_2 content. In this study, the numerical melting model of Brophy (2008) was modified in two important ways. First, because the Asago amphibolites do not contain quartz, it was removed as a melting phase. Second, the observed accessory minerals (sphene, apatite and zircon) have been added to the melting history. Their initial abundances have been set at sphene (0.5 %), apatite (0.15 %) and zircon (0.05 %), which represent their average observed modal abundances in the amphibolites. It is further assumed that all accessory minerals are

completely refractory throughout the amphibolite melting. Table 2 summarizes the overall numerical melting model employed. The SiO_2 -dependant REE D values for all major minerals are the same as those used by Brophy (2008). D values for the accessory minerals are based on the published sets of Fujimaki (1986) (apatite), Luhr et al. (1984) (sphene) and Sano et al. (2002) (zircon). These particular sets were chosen because, for each mineral, they represent (1) an overall D value pattern representative of that established from multiple data sets (i.e., concave upwards, concave downwards) and (2) the highest overall D values. In all cases, D values for any missing elements were estimated by interpolation and the overall D value profiles were then “smoothed” to remove any irregularities.

Table 2 Amphibolite melting model

	Stage I	Stage II	Stage III	Stage IV	
Modal abundance—% melting variation					
hbd	43.7	15.9	0	0	0
plag	49.7	47.6	44.6	29.7	0
cpx	0	13.9	22.8	19.8	0
opx	0	5	9.9	4.9	0
mag	4	5	4	3	0
ilm	2	2	2	2	0
Sphene	0.5	0.5	0.5	0.5	0
Apatite	0.15	0.15	0.15	0.15	0
Zircon	0.05	0.05	0.05	0.05	0
Melt	0	10	16	40	100
Liquid SiO ₂ —% melting variation					
Batch melting – wt% SiO ₂ = 76.035 – 0.35055(x) + 0.005361(x) ² – 0.00021826(x) ³					
Fractional melting—wt% SiO ₂ = 76.504 – 0.73607(x) + 0.01818(x) ² – 0.00088319(x) ³					
x = Wt% melting					

Figure 10 shows the modeled variations in liquid REE abundance (chondrite-normalized) as a function of liquid SiO₂ content for all of the REE for which natural abundance data are available. Results are shown for both batch and fractional melting and cover liquid compositions ranging from 60 to 76 % SiO₂. Also shown are observed abundances for the mafic amphibolites and felsic veins. Eu was not modeled due to the uncertainty in Eu *D* values (Brophy 2008). The modeled variations assume initial abundances (*C*₀) equal to the average of the mafic amphibolite samples. Because the felsic veins are plotted on an anhydrous SiO₂ basis, they all plot at SiO₂ contents >76 % SiO₂. A comparison of the model and observed REE abundances in the felsic veins shows excellent agreement for the MREE and HREE (Sm–Yb), but rather poor agreement for the LREE (La–Nd) where observed abundances are higher than the predicted values.

Discussion

The Brophy (2008) model had two specific predictions. First, all of the REE should display negative REE–SiO₂ correlations for liquid SiO₂ greater than around 65 wt%, and second, the REE abundances in very SiO₂-rich liquids (around 75–76 % SiO₂) should be the same or less than those in the source rock (i.e., *C*_l/*C*₀ ≤ 1). Figure 10 shows that the natural felsic samples cover a very narrow range of SiO₂ content (76–81 % on an anhydrous basis) and therefore cannot be used to assess a negative (or positive) REE–SiO₂ variation. Thus, the first of Brophy's (2008) model

predictions cannot be evaluated. However, Fig. 10 does show that, with the exception of the LREE, all of the natural felsic rocks display REE abundances that are the same or less than those in the mafic amphibolites. Furthermore, with the exception of the LREE, the predicted model values agree very well with the observed abundances in the felsic veins, thus confirming, in general, the second of Brophy's (2008) model predictions. Nevertheless, the discrepancy between the predicted and observed values for the LREE cannot be ignored, and this is turned to now.

Figure 11a shows a range of predicted REE profiles for a model 76 % SiO₂ melt. The individual REE profiles were constructed by combining the model enrichment factors for (*C*_l/*C*₀) for a 76 % SiO₂ model melt with the corresponding initial element values in each of the natural amphibolites (*C*₀). Figure 11b compares this range with the observed profiles in the felsic veins. The results further highlight the discrepancy for the LREE and the good agreement for the MREE to HREE. What would be required to explain the discrepancy would be an amphibolite source rock that is LREE-enriched relative to ones in which the felsic veins currently reside. It is important to recall that the felsic veins most likely are the result of partial melting of some other amphibolite source rock presumably nearby and perhaps at a greater depth. Thus, it is possible that some other amphibolite that contains the required LREE-enriched signature could have been the actual source rock.

Figure 12 shows the REE profiles reported by Suda (2004) for a moderate number of amphibolites from the Asago body of the Yakuno amphibolites. The amphibolites turn out to be of two types. The first type, referred to here as Group 1 amphibolites, has flat to slightly convex profiles with chondrite-normalized values ranging from around 10 to 50. These features are similar to those of the amphibolites sampled in this study. Significantly, the second type (Group 2 amphibolites) displays a fractionated profile with moderate LREE enrichment relative to the Group 1 amphibolites. In Fig. 13, the five group 2 amphibolites of Suda (2004) have been used as the amphibolite source rock to, once again, calculate a range of REE profiles for a model 76 % SiO₂. When these results are compared with the observed felsic veins, one sees perfect agreement for all elements including the LREE. Thus, if one were to assume that the true source rock for the felsic veins was an amphibolite with REE abundances similar to the group 2 amphibolites, then both of Brophy's (2008) theoretical predictions are completely confirmed.

Conclusions

The main goal of this study was to evaluate the REE–SiO₂ systematics predicted by Brophy (2008) for the formation

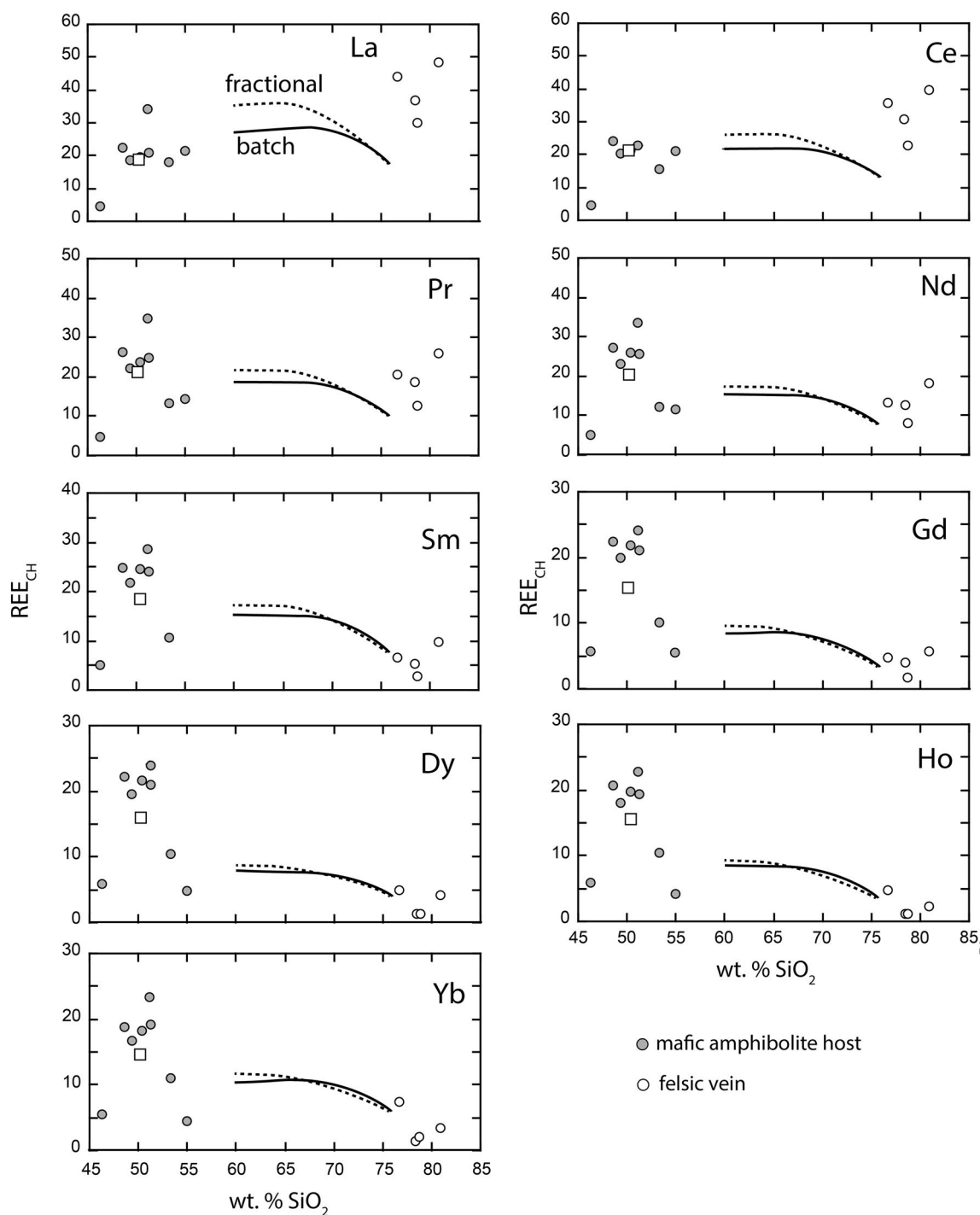


Fig. 10 Calculated chondrite-normalized REE-SiO₂ variations for batch melting (solid curve) and fractional melting (dashed curve). Also shown are the host amphibolites (filled circles) and felsic veins (open circles). For each element, the initial concentration is indicated

by the open square, which represents the average of all mafic amphibolite host samples. Model results are shown only for SiO₂ contents ranging from 60 to 76 wt%

of island arc felsic magma through the dehydration melting of lower island arc crust amphibolite. Specifically, it has been proposed that, for liquids greater than around

63 wt% SiO₂, dehydration melting of amphibolite should yield decreasing REE abundances with increasing liquid SiO₂. This is in contrast to the fractional crystallization

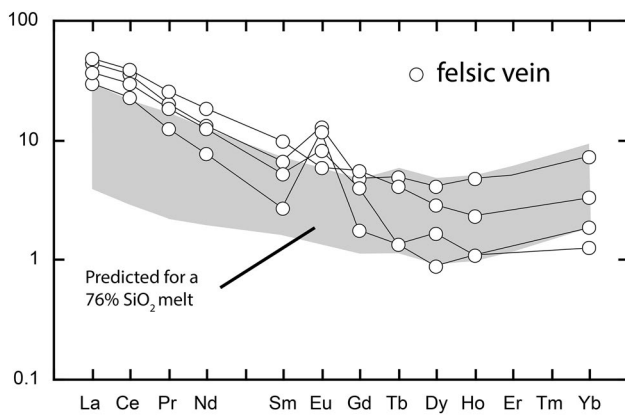


Fig. 11 Comparison of observed chondrite-normalized REE profiles in the felsic veins with a range of calculated REE profiles for 76 % SiO_2 liquids generated by the partial melting of individual mafic amphibolite host samples (*shaded region*)

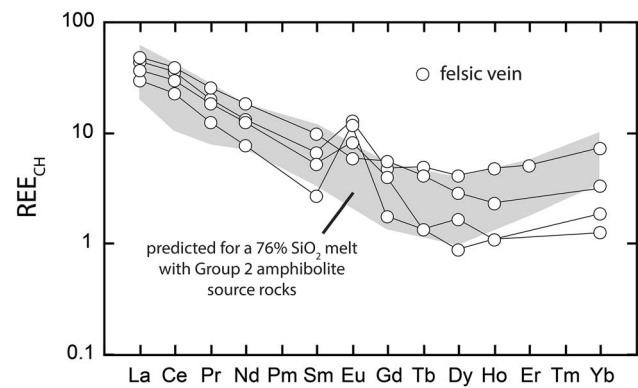


Fig. 13 Comparison of the range of calculated chondrite-normalized REE profiles for a 76 % SiO_2 liquid using the Group 2 amphibolites of Suda (2004) as source rocks (*shaded region*), with the observed range of abundances in the felsic veins

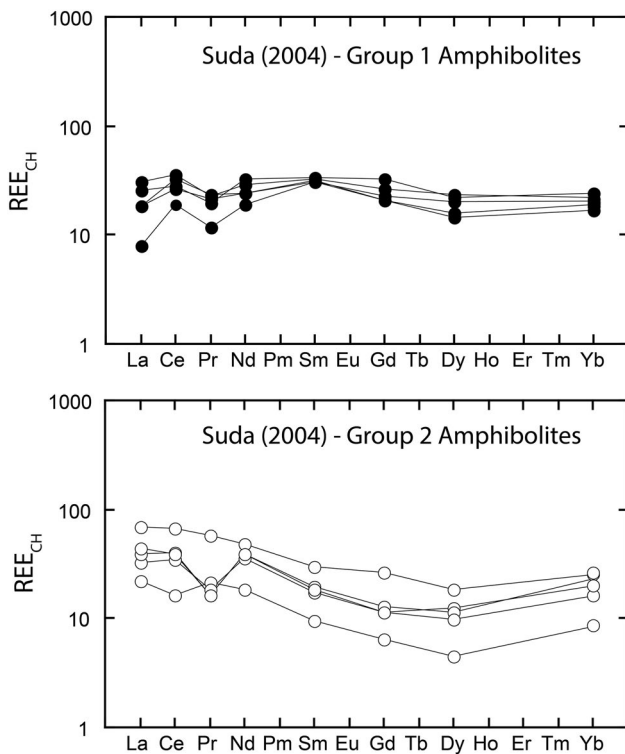


Fig. 12 Chondrite-normalized REE abundances reported by Suda (2004) for several amphibolites in the Asago body. Group 1 amphibolites have relatively flat but slightly concave upwards profiles, while Group 2 amphibolites have fractionated profiles with moderate LREE enrichment

of IAB magma (unless significant amounts of hornblende fractionation are involved), which should yield increasing REE abundances with liquid SiO_2 . If the modeling is correct, then the contrasting behavior of REE with increasing liquid SiO_2 could provide a simple test for discerning

a fractional crystallization versus partial melting origin for natural island arc felsic magmas. The Permian-age Asago body in the Yakuno Ophiolite, located on Honshu island, Japan, contains an example of amphibolite migmatites containing highly felsic believed to be generated by dehydration melting of amphibolite (Suda 2004). This field locality has been used to verify the presence or absence of the predicted REE– SiO_2 systematics in natural plagiogranites. The results indicate that, if the source rock for the felsic is similar to a LREE-enriched amphibolite known to exist in the Asago body (Suda 2004), then all facets of the REE– SiO_2 systematics predicted by Brophy (2008) are confirmed. Based on these findings, it is suggested that REE– SiO_2 systematics can be used to distinguish between a fractional crystallization and partial melting origin for natural island arc felsic magmas.

References

- Beard JS, Lofgren GL (1991) Dehydration melting and water saturated melting of basaltic and andesitic greenstones and amphibolites. *J Petrol* 29:36–51
- Brophy JG (2008) A study of rare earth element (REE)– SiO_2 variations in felsic liquids generated by basalt fractionation and amphibolite melting: a potential test for discriminating between the two different processes. *Contrib Mineral Petrol* 156:337–357
- Brophy JG, Ota T, Kunihiro T, Tsujimori T, Nakamura E (2011) In situ ion-microprobe determination of trace element partition coefficients for hornblende, plagioclase, orthopyroxene and apatite in equilibrium with natural rhyolitic glass, Little Glass Mountain Rhyolite, California. *Am Mineral* 96:1838–1850
- Dalpe C, Baker DR (2000) Experimental investigation of large ion lithophile element, high field strength element, and rare earth element partitioning between calcic amphibole and basaltic melts; the effects of pressure and oxygen fugacity. *Contrib Mineral Petrol* 140:233–250
- Davidson J, Turner S, Handley H, MacPherson C, Dosseto A (2007) Amphibole “sponge” in arc crust? *Geology* 35:787–790

- Davidson J, Turner S, Plank T (2013) Dy/Dy*: variations arising from mantle sources and petrogenetic processes. *J Petrol* 54:525–537
- Deering CD, Cole JW, Vogel TA (2008) Magmatic evolution and distribution in the Taupo volcanic zone, New Zealand. *Geochim Cosmochim Acta* 72:70–73
- Fujimaki H (1986) Partition coefficients of Hf, Zr and REE between zircon, apatite and liquid. *Contrib Mineral Petrol* 94:42–45
- Hayasaka Y (1990) Maizuru terrane. In: Ichikawa Y, Mizutani S, Hara I, Hada S, Yao A (eds) Pre-Jurassic evolution of Eastern Asia, pre-Cretaceous terranes of Japan. Publication of IGCP project no 224, Osaka City University, Osaka, pp 81–95
- Ichiyama Y, Ishiwatari A (2003) Petrochemical evidence for off-ridge magmatism in a back-arc setting from the Yakuno ophiolite, Japan. *Island Arc* 13:157–177
- Ishiwatiri A (1985) Granulite-facies metacumulates of the Yakuno ophiolite, Japan: evidence for unusually thick oceanic crust. *J Petrol* 26:1–30
- Klein M, Stosch HG, Seck HA (1997) Partitioning of high field strength and rare earth elements between amphibole and quartz-dioritic to tonalitic melts: an experimental system. *Chem Geol* 138:257–271
- Leake BE, Wooley AR, Arps CES, Birch WD, Gilbert MC, Grice JD, Hawthorne FC, Kato A, Kisch HJ, Krivovichev VG, Linthout K, Lard J, Mandarino J (1997) Nomenclature of amphiboles: report of the subcommittee of the international mineralogical association, commission on new minerals and mineral names. *Mineral Mag* 61:295–321
- Luhr JF, Carmichael ISE, Varekamp JC (1984) The 1982 eruption of El Chichon Volcano, Chiapas, Mexico: mineralogy and petrology of the anhydrite bearing pumices. *J Volcanol Geotherm Res* 23:69–108
- McDonough WF, Sun SS (1995) The composition of the Earth. *Chem Geol* 120:223–253
- Rapp RP, Watson EB (1995) Dehydration melting of metabasalt at 8–32 kbar: implications for continental growth and crust-mantle recycling. *J Petrol* 36:891–931
- Rushmer T (1991) Partial melting of two amphibolites: contrasting experimental results under fluid-absent conditions. *Contrib Mineral Petrol* 107:41–59
- Sano Y, Terada K, Fukuoka T (2002) High mass resolution ion microprobe analysis of rare earth elements in silicate glass, apatite and zircon: lack of matrix dependency. *Chem Geol* 184:217–230
- Sawyer EW (2008) Atlas of migmatites. The Canadian Mineralogist, Special Publications, vol 9. NRC Research Press, Ottawa, 371 pp
- Sisson TW (1994) Hornblende-melt trace element partitioning measured by ion microprobe. *Chem Geol* 117:331–344
- Suda Y (2004) Crustal anatexis and evolution of granitoid magma in Permian intra-oceanic island arc, the Asago Body of the Yakuno ophiolite, southwest Japan. *J Mineral Petrol Sci* 97:339–356